Journal of Visualization, Vol. 1, No. 1 (1998) 9-28

Flow Visualization of Relaminarization Phenomena in Curved Pipes and the Related Measurements

Kurokawa, M.*, Cheng, K. C.*, and Shi, L.*

* Department of Mechanical Engineering, University of Alberta, Edmonton, Alberta, Canada.

Received 23 October 1997.
Revised 17 December 1997.

***Abstract*:** Flow visualization results for secondary flow phenomena at the exit of 90° and 180° bends and helically coiled pipes (1, 2 and 5 turns), (radius of curvature R_c = 381 mm, inside pipe diameter d=37.5 mm, curvature ratio $d/2R_c$ = 0.049) and in the downstream straight pipe (l/d = 30) are presented to study the stabilizing (relaminarization) effect in curved pipes with fully developed entry turbulent air flow and the destabilizing (re-transition from laminar to turbulent flow) effect in the downstream straight region. The entry Reynolds numbers are Re = 2200, 3200, 4300 and 5300).

The related measurement results using a hot-film anemometer are presented for developing profiles of the time-mean streamwise velocity distribution and the axial turbulence intensity field in the 180° return bend and in the downstream straight pipe for Reynolds numbers Re = 3200, 4300, 6300 and 8200.

The time traces showing the output of the hot-film sensor are also presented for developing fluctuating velocity field in the 180° bend and in the downstream straight pipe for the same Reynolds number range. Some aspects of the relaminarization phenomena in curved pipes and the re-transition phenomena from laminar to turbulent flow in the downstream straight pipe are clarified by the present experimental investigation.

***Keywords*:** laminarization, curved pipes, visualization, measurements.

Nomenclature:

a	inside pipe radius, $d/2$
d	inside pipe diameter, $2a$
K	Dean number, $Re\ (a/R_c)^{1/2}$
l	downstream tube length
R_c	radius of curvature for bend or coil
Re	Reynolds number, $u_m d\ /\ v$
u	time-mean local axial velocity
u'	fluctuating axial velocity component
u_m	mean velocity across the cross-section
x,y	horizontal and vertical coordinates (Fig.3)
z	axial coordinate in downstream pipe
v	kinematic viscosity of air
θ	bend or coil turn angle

1. Introduction

Internal fluid flows in pipes and ducts with secondary flow caused by such body forces as centrifugal, buoyancy and Coriolis forces are somewhat analogous (Trefethen, 1957; Ishigaki, 1996) and form a class of technologically important problems. Extensive experimental and theoretical research has been conducted into the fluid mechanics of such problems in recent years and the literature is very extensive. The present investigation is concerned with flow transition phenomena involving laminarization of turbulent flow in curved pipes, bends and helically coiled pipes with upstream and downstream straight pipe air flows.

In the experimental arrangement a low Reynolds number turbulent air flow was passed through a hydrodynamic development section with a sufficiently long straight pipe (based on entry length for turbulent flow) to obtain fully developed turbulent flow and thence into the curved pipes with straight downstream pipes.

The effects of secondary flow on laminarization of turbulent flow in curved pipes consisting of 90° bend, 180° return bend, 360° bend and helically coiled pipes with 2 and 5 turns were investigated by flow visualization using smoke injection technique and by hot-wire anemometry measurement. Horizontal and vertical distributions of turbulence intensity and time-mean velocity were measured for various Reynolds numbers and downstream positions.

Of particular interest is the reverse transition (turbulent-laminar) for flow through a curved pipe and laminar-turbulent transition in a straight downstream pipe. Reynolds number (inertia force over viscous force) has a destabilizing effect for flow transition in a straight pipe and secondary flow in a curved pipe has a stabilizing effect to delay the transition from laminar to turbulent flow. Apparently the delay of laminar-turbulent transition in curved pipes is closely related to the relative importance between Reynolds number and secondary flow intensity due to centrifugal forces.

A brief review of the existing literature on laminarization of turbulent flow in curved pipes is in order. Flow and heat transfer characteristics for both laminar and turbulent flows in curved pipes relating to developing and fully developed velocity and temperature profiles, friction factor, and Nusselt number are well reviewed by Ackeret (1967), Ward-Smith (1980), Berger et al. (1983), Nandakumar and Masliyah (1986), Ito (1987), and Berger (1991).

It has been known since the works of Taylor (1929) and White (1929) that the effect of curvature in curved pipe flow is to increase the critical Reynolds number denoting the transition from laminar to turbulent flow above that for flow in a straight pipe. Flow visualization experiments are described by Taylor (1929) in which coloured fluid is introduced through a small hole in the side of a glass helix through which water is running; the secondary flow circulation in the cross-section of a curved pipe is observed. Taylor (1929) observes that in a pipe bent into a helix the diameter of which was 18 times that of the cross-section, steady stream-line motion persisted up to a Reynolds number, 5830, i.e. 2.8 times Reynolds' criterion for a straight pipe flow. This occurred in spite of the fact that the flow was highly turbulent on entering the helix. White's resistance measurements (1929) also reached the conclusion that a higher speed of flow is necessary to maintain turbulence in a curved pipe than in a straight one. Thus Taylor (1929) and White (1929) discovered the laminarization phenomena in curved pipe flows.

The experimental data indicating the first appearance of turbulence are presented as Fig.3 in Taylor (1929). A number of empirical equations for critical Reynolds number based on pressure-drop measurements are reviewed by Ward-Smith (1980) and Nandakumar and Masliyah (1986). Ito (1959) gives the equation:

$$(Re)_{cr} = 2 \times 10^4 \left(\frac{a}{R_c}\right)^{0.32} \qquad \text{for } 10 < \frac{R_c}{a} < 860 \tag{1}$$

Ito's equation predicts a critical Reynolds number of 2300 to occur when $R_c / a = 862$ and one may infer that for values of $R_c / a > 862$, the critical Reynolds number is taken as that for straight pipe flow.

Sreenivasan and Strykowski (1983) describe the experiments on the stabilization effects in flow through helically coiled pipes and in a long straight section downstream. The flow visualization of laminarization in coiled pipes (pipe diameter = 1.91 cm, radius of curvature R_c = 9.0 cm, Re = 4050) obtained by dye-injection method for water flow by Viswanath et al. (1978) is shown to demonstrate the phenomena of laminarization. The determination of the critical Reynolds numbers from the oscillograms of hot-wire traces at locations about (0.25a) from the inner and outer walls taken at 2½ coils into the helix (dia.= 1.905 cm, R_c = 16.51 cm) is shown. The experimental data on critical Reynolds number for flow in helically coiled pipes are of special interest.

General review on relaminarization was presented by Narasimha (1977), Narasimha and Sreenivasan (1979) and Sreenivasan (1982, 1983). Further discussion on relaminarization phenomena in curved pipes can be found in Ito (1978), Kalb and Seader (1983), Anwer et al. (1989) and Humphrey and Webster (1993). Further references

related to the present investigations are noted here: Rowe (1970), Patankar et al. (1974, 1975), Chang et al. (1983), Cheng and Yuen (1987), Ohadi and Sparrow (1987, 1990a, 1990b), Akiyama et al. (1988) and Cheng et al. (1995).

The transition from turbulent to laminar gas flow can occur in a heated pipe and the relaminarization phenomenon is discussed by Bankston (1970), Torii and Yang (1997) and many other investigators. Laminarization of turbulent pipe flow by fluid injection and transpiration are discussed by Pennell et al. (1972) and Lombardi et al. (1974). It is seen that laminarization of turbulent flow can occur under the action of various body forces in internal flow problems.

Apparently secondary flow observed in a curved pipe plays an important role in laminarization process, and a remark about its formation may be in order. The secondary flow pattern depends on the magnitude of Dean number. At higher Dean number, centrifugal forces dominate in the core region of the circular cross-section. The strength of a local centrifugal force depends on its distance from the center of curvature and the main velocity. Along the horizontal symmetric axis of the cross-section, the centrifugal force increases from zero at the inner wall to the maximum value and is zero at the outer wall. On the other hand, the pressure increases monotonically from the inner wall toward the outer wall. The pressure gradient in the central core is caused by centrifugal forces. It is then clear that the region near the outside bend is unstable and the region near the inside bend is stable for fully developed flow. Thus Dean's instability problem in a curved pipe or a curved square duct may arise with the formation of an additional pair of counter-rotating vortices (Dean vortices) at Dean number around 100. The distribution of the centrifugal force across the cross-section leads to the emergence of a secondary flow which is directed outwards in the centre and inwards towards the center of curvature near the wall.

The influence of curvature is stronger in laminar than in turbulent flow. The flow phenomena in a curved pipe may be regarded as a combination of the main flow with a secondary flow at right angles to it. The secondary flow in a curved pipe is known as Prandtl's secondary flow of the first kind. The secondary flow has the effect of displacing the region of maximum velocity closer to the outer concave wall. The destabilizing effect of concave wall and the stabilizing effect of convex wall for flow in curved channels are discussed by Prandtl (1935).

The laminarization of turbulent flow in curved pipes is apparently the resulting state of affairs caused by the flow phenomena near the convex and concave walls. The secondary flow extracts its kinetic energy from the main flow, and suppresses the turbulence. Consequently, the onset of turbulence is delayed.

Under normal conditions, the transition Reynolds number for flow in a smooth pipe is in the range Re = 2300~4000. It is noted that our present knowledge on flow transition in curved pipes is rather limited in comparison with that in straight pipes and ducts.

2. Experimental Apparatus and Procedure

Figure 1 shows a schematic diagram of the experimental apparatus, which consists of a test section (180° bend), an entrance straight copper pipe (diameter d = 37.5 mm, 6.3 m long), and an air supply system. The building compressed air free of water and oil was used. The test section (90° and 180° bends, one-turn (360° bend), two-turn and five-turn helically coiled pipes) with coil diameter $2R_c$ = 762 mm, pitch 127 mm) was placed in the horizontal configuration.

The entry pipe (l/d = 168) is long enough to serve as a hydrodynamic development section to obtain fully developed turbulent entry flow to the curved test section. Three kinds of straight copper pipe with length $10d$, $20d$ and $30d$ serve as the downstream test section after the curved test section. The curved pipe was made from a commercially available rolled soft copper pipe with an average inside diameter d = 37.5 mm and a radius of curvature R_c = 381 mm. Thus the curvature ratio is a/R_c = 0.0492. The cross-section of the curved pipe was not perfectly circular due to the coiling process, but the result of inside diameter measurements at the inlet and exit of the curved section showed that the distortion of the cross-section was relatively small and the deviation from the average inside diameter was within 2 percent.

The building compressed air flows horizontally through a control valve, an air filter, a pressure regulator, air tank, a laminar flow element, a settling chamber, an entrance straight pipe, the curved pipe (test section) and the straight downstream test pipe in succession. The air flow rate was measured by the *Meriam* laminar flow element together with a calibrated differential pressure transducer. The calibration curve of the laminar flow element for flow rate was also verified by a standard gas flow meter.

Figure 2 shows the 180° bend test section and the downstream test section. Figure 3 illustrates the coordinate system at the exit of the curved pipe and the locations A, B, C and D.

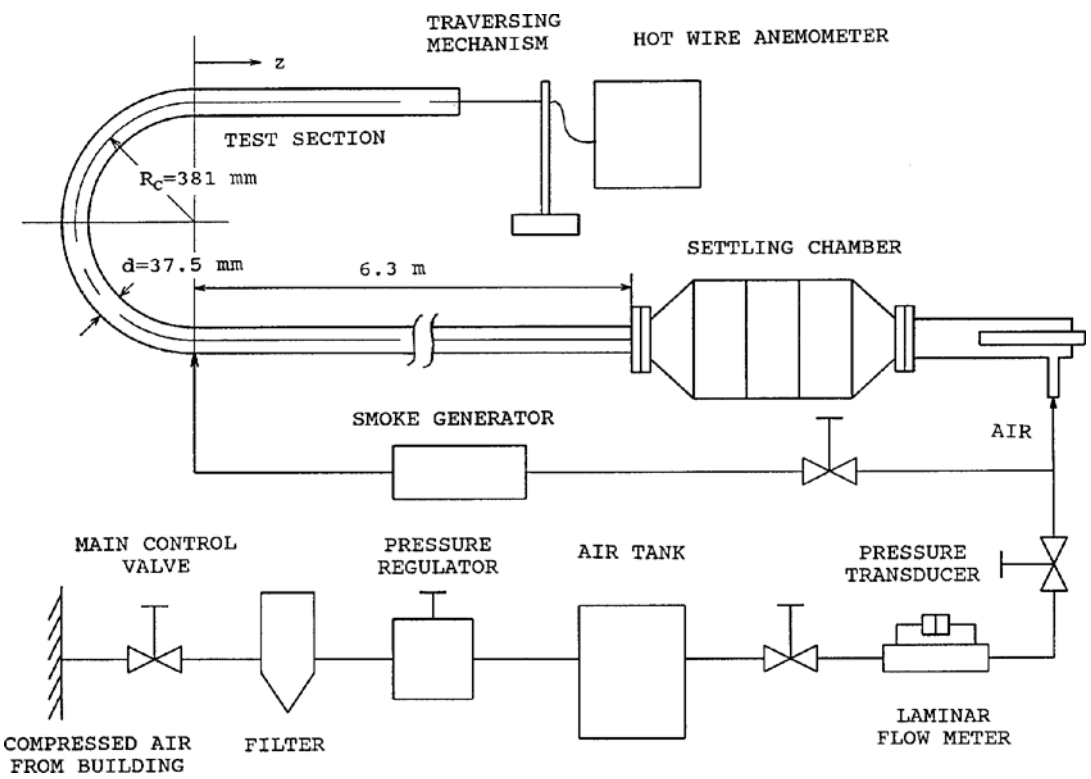

Fig. 1. Schematic diagram of experimental apparatus.

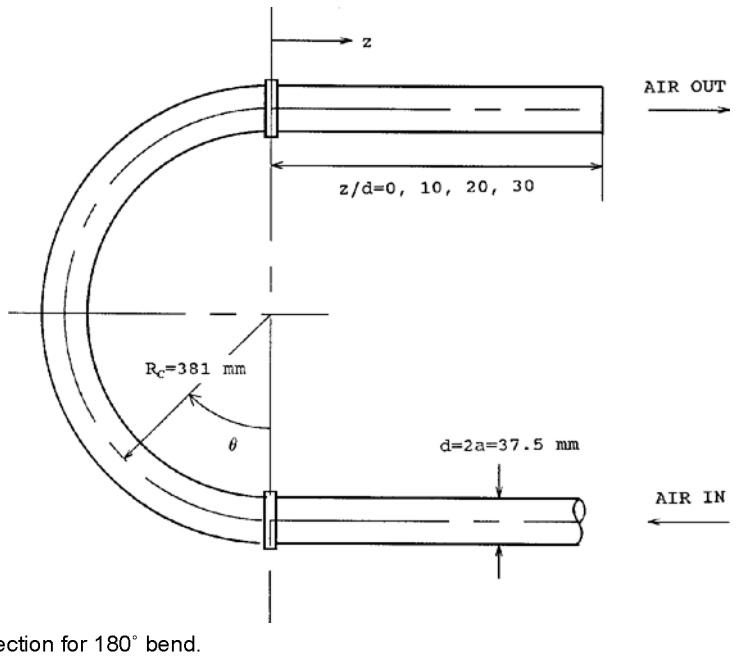

Fig. 2. Test section for 180° bend.

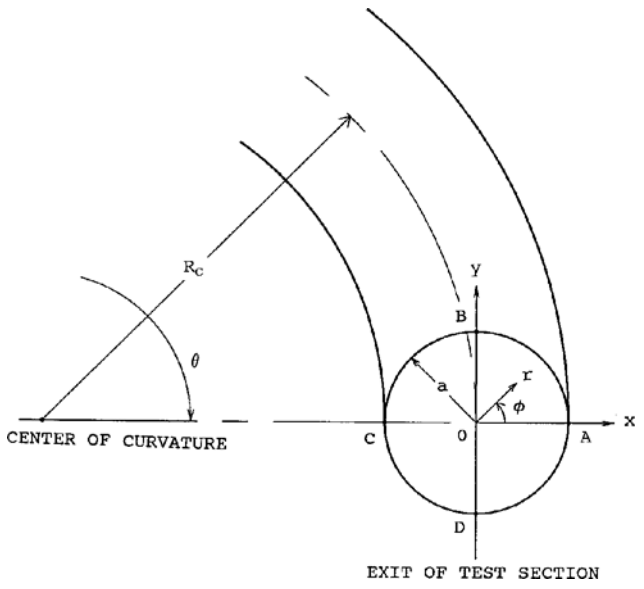

Fig. 3. Coordinate system at the exit of bend test section.

2.1 Flow Visualization Experiments

For flow visualization of secondary flow patterns at the exit of the curved test section and the downstream straight pipe positions at z/d = 10, 20 and 30, a smoke injection method was used. The smoke generated by burning Chinese incense sticks in the smoke generator was injected through the smoke injection section with four small holes (1.5 mm in diameter) equally spaced along the periphery. The smoke injection section with the same inside diameter as the test section was installed between the exit of the entrance straight pipe and the inlet of the test bend or the helical coil (see Fig.1). In order to obtain the cross-sectional view of the secondary flow, the sheet of light was produced from a 2.0 kW Xenon illuminator light source.

Visualization pictures were taken with a *Nikon FM*-2 single lens reflex camera with 50 mm micro-lens using *Kodak TRI-X* black and white film. The camera setting was f 3.5 and the shutter speed was 1/4 to 1 sec. It is noted that the flow visualization technique used is most simple.

2.2 Measurements

Local measurements were made to determine the axial turbulent velocity fluctuations and the time-mean axial velocity along the horizontal and vertical axes of the cross-section (see A-C and B-D as shown in Fig.3). The measurements were performed at five positions including the inlet and exit of the bend section and the downstream positions in the straight pipe at z/d = 10, 20 and 30. The data were acquired with the aid of a *Thermosystems model-1050* hot-film sensor (alumina coated platinum film sensor on glass rod, length 2 mm and 0.051 mm diameter) used in conjunction with a *Thermosystems* constant temperature anemometer. The output signal from the anemometer was processed by the *HP* data acquisition system with the *HP* personal computer. The sampling rate of the analog to digital converter was set at about 10 Hz.

A traversing mechanism with the smallest division of 0.1 mm was used to hold the hot-film sensor support. The hot-film sensor was calibrated against a standard Pitot tube for turbulent flow in pipe in the velocity range 1.5 to 10 m/s. For a fully developed laminar flow (parabolic velocity profile) in a circular pipe, the centre velocity is $2u_m$ (u_m = average velocity). This relation was used in the calibration of the sensor in the velocity range below 1.5 m/s. Thus the hot-film sensor was also calibrated against the centre velocity of a fully developed laminar pipe flow. The corresponding outputs from the linearizer of the anemometer could be fitted to three straight lines by a least square method with an error of less than 2 percent. The probe and traversing mechanism were introduced into the flow from the exit end of the pipe. The experimental data were reduced by means of a hybrid computer in on-line operation. Specifically, at each probe location the computer output provided the time-mean axial velocity and the root-mean-square value of the fluctuations in the axial velocity.

3. Experimental Conditions

The operating conditions of the experiments were characterized by the entrance Reynolds number at the inlet of the curved pipe and the type of the bend or helical coil test section. The experimental conditions for flow visualizations and measurements are listed in Tables 1 and 2, respectively. Tables 1 and 2 also show the scope of the present investigation.

Table 1 Experimental conditions for flow visualizations.

Curvature Ratio, a / R_c	0.049
Bend Angle, θ	90, 180, 360, 720, 1800 degree
Reynolds Number, Re	2200, 3200, 4300, 5300
Dean Number, K	480, 720, 950, 1170
Axial Positions, z / d	0, 10, 20, 30

Table 2 Experimental conditions for measurements.

Curvature Ratio, a / R_c	0.049
Bend Angle, θ	180 degree
Reynolds Number, Re	3200, 4300, 6300, 8200
Dean Number, K	720, 950, 1390, 1820
Axial Positions, z / d	Inlet to the Bend, 0, 10, 20, 30

4. Results and Discussion

4.1 Laminarization Phenomena in Curved Pipes

For fully developed flow in a straight smooth pipe, laminar - turbulent transition occurs in the Reynolds number range Re = 2300 to 2700 depending on the entrance condition. The smoke injection technique reveals the cross-sectional view of the secondary flow pattern for laminar flow regime only. For turbulent flow, smoke diffusion due to mixing occurs and the secondary flow pattern cannot be seen. Thus the region of flow field with laminarization is revealed by the appearance of the secondary flow.

For the present problem, a fully developed turbulent flow from a straight upstream pipe enters the circular-arc bend with bend or turn angle θ = 90, 180, 360 (1-turn), 720 (2-turn) or 1800 (5-turn) degree. The flow then enters a straight downstream pipe attached to the bend section. In the experimental arrangement one has hydrodynamic entrance region problem with laminarization process in both the curved and straight sections.

The photographic results of the secondary flow patterns at the axial distances z/d = 0, 10, 20 and 30 in a downstream straight pipe are shown in Figs. 4 to 8 for Reynolds numbers

Re = 2200, 3200, 4300 and 5300 respectively. The corresponding Dean numbers are K = 488, 710, 954 and 1176, respectively. The right-hand side of each photograph for z/d = 0 represents the outer wall (point A in Fig.3).

The Case of 90° Bend ($R_c\theta / d$ = 15.95), Fig.4

At Re = 2200 (K = 488), the secondary flow at the exit of 90° bend can be seen near the outer wall. The secondary flow represents the stabilizing effect of the centrifugal forces in the core region. Judging from the rather weak secondary flow, one concludes that the entry flow to the 90° bend is a fully developed turbulent flow. The development of secondary flow consisting of a pair of counter-rotating vortices continues in the downstream section. At z/d = 30, one sees clearly the boundary layer for secondary flow along the side and inner walls.

At Re = 3200 (K = 710), a weak secondary flow can been seen near the outer wall at the exit of the bend.

The laminarization process is considered to be weak in the bend. At $z/d = 10$, the secondary flow is still discernible near the outer wall. At $z/d = 20$ and 30, one sees the retransition to a turbulent flow. At $Re = 4300$ ($K = 954$), the secondary flow is quite weak at $z/d = 0$ and 10. At $z/d = 20$ and 30, the flow becomes turbulent again. No secondary flow can be seen due to smoke diffusion in turbulent flow.

At $Re = 5300$ ($K = 1176$), a weak secondary flow may exist near the outer wall for the section $z/d = 0$. Further downstream, the turbulent flow returns since one cannot detect the secondary flow. At each axial position, the degree of laminarization decreases with the increase of the Reynolds or Dean number. It is clearly seen that the intensity of the secondary flow represents the stabilizing effect of the centrifugal forces and shows the laminarization process caused by curvature. For 90° bend, the laminarization is weak because of the shorter axial distance.

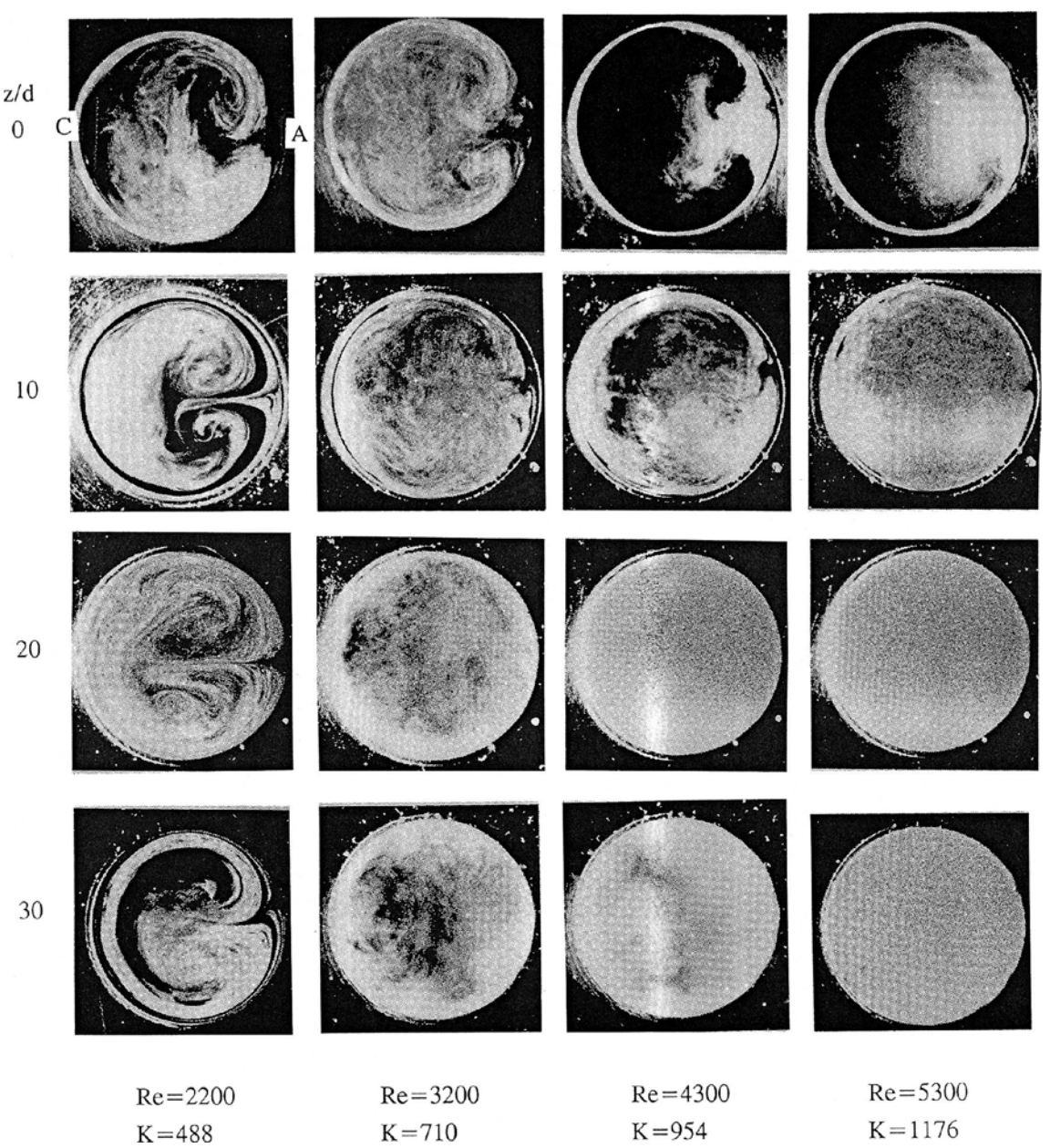

Fig. 4. Developing secondary flow patterns for 90° bend and downstream straight pipe.

The Case of 180° Bend ($R_e\theta / d = 31.9$), Fig.5

In the literature the case of flow in a 180° return bend has been studied rather extensively for both laminar and turbulent flows. At *Re* = 2200 and 3200, the appearance of the secondary flow near the outer wall at the exit of 180° bend and subsequent gradual decay of its intensity in the downstream section are quite clear. At *Re* = 4300 and 5300, the secondary flow at the exit of the bend is seen to be quite weak and the return to turbulent flow in the downstream straight section can be seen clearly. No secondary flow revealed by smoke injection method in the cross-section means turbulent flow. However, the secondary flow exists for turbulent flow in a curved pipe. It is noted that the smoke injection method reveals the laminarization phenomenon.

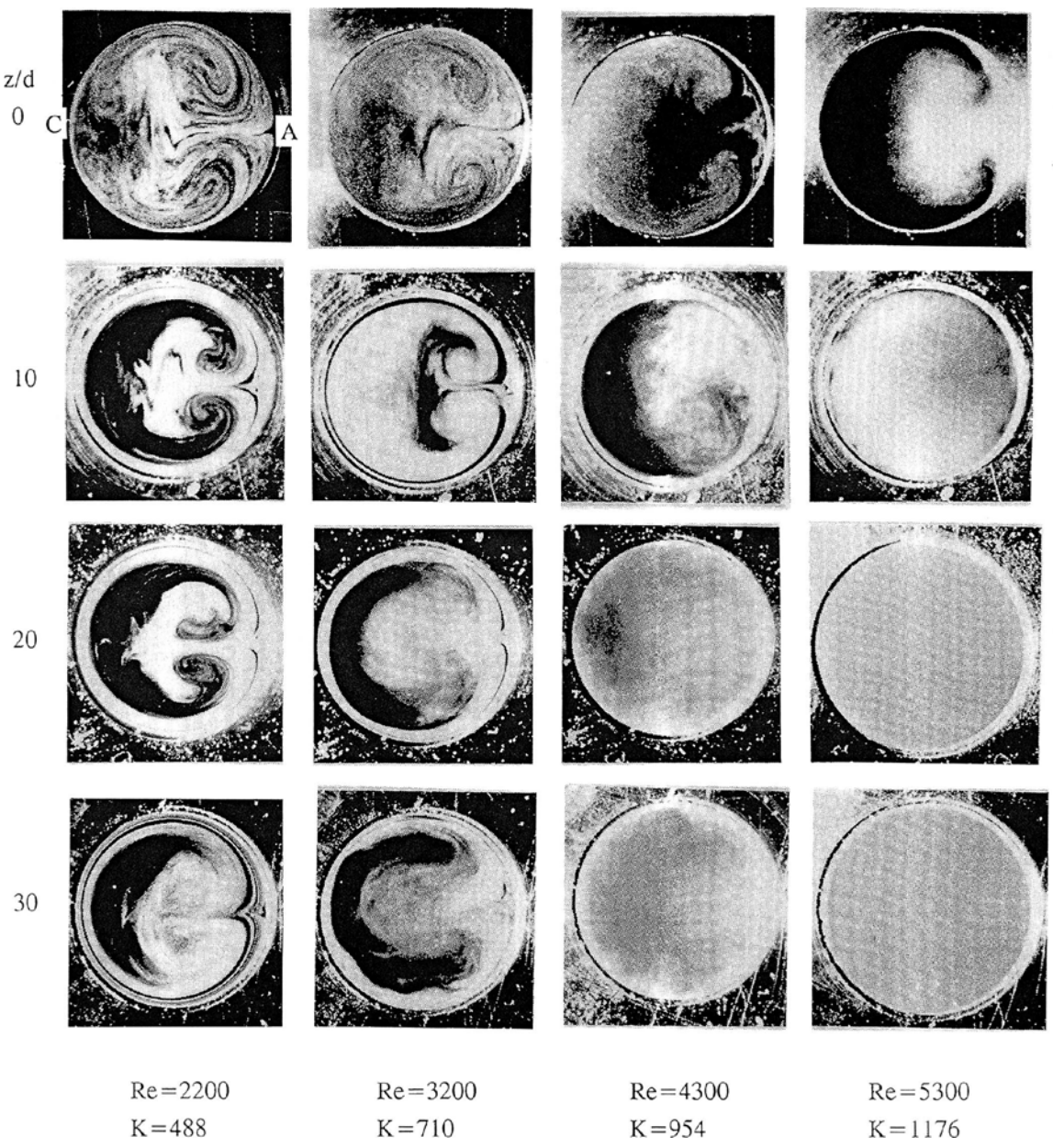

Fig. 5. The case of 180° bend.

The Case of 360° Bend ($R_c\theta / d = 63.8$), Fig.6

The developing flow in curved pipes with a fully developed low-Reynolds number turbulent flow is quite different from the development of turbulent flow in curved pipes with the mean axial velocity exceeding the critical velocity for laminar - turbulent transition because of the laminarization process.

At $z/d = 0$, the intensity of secondary flow decreases with the increase of Reynolds number. At $Re = 5300$, the secondary flow exists near the inner wall. The secondary flow pattern at $Re = 2200$ suggests that the flow may become fully developed at the exit of one-turn coil and the relaminarization process ends. With $Re \geq 3200$ the laminarization still continues after one turn. Apparently the secondary flow persists in the downstream section for $Re = 2200$ and 3200 before its complete disappearance in further downstream. For $Re = 4300$, the laminar secondary flow disappears at $z/d = 30$. At $Re = 5300$, the flow becomes turbulent again at $z/d = 10$.

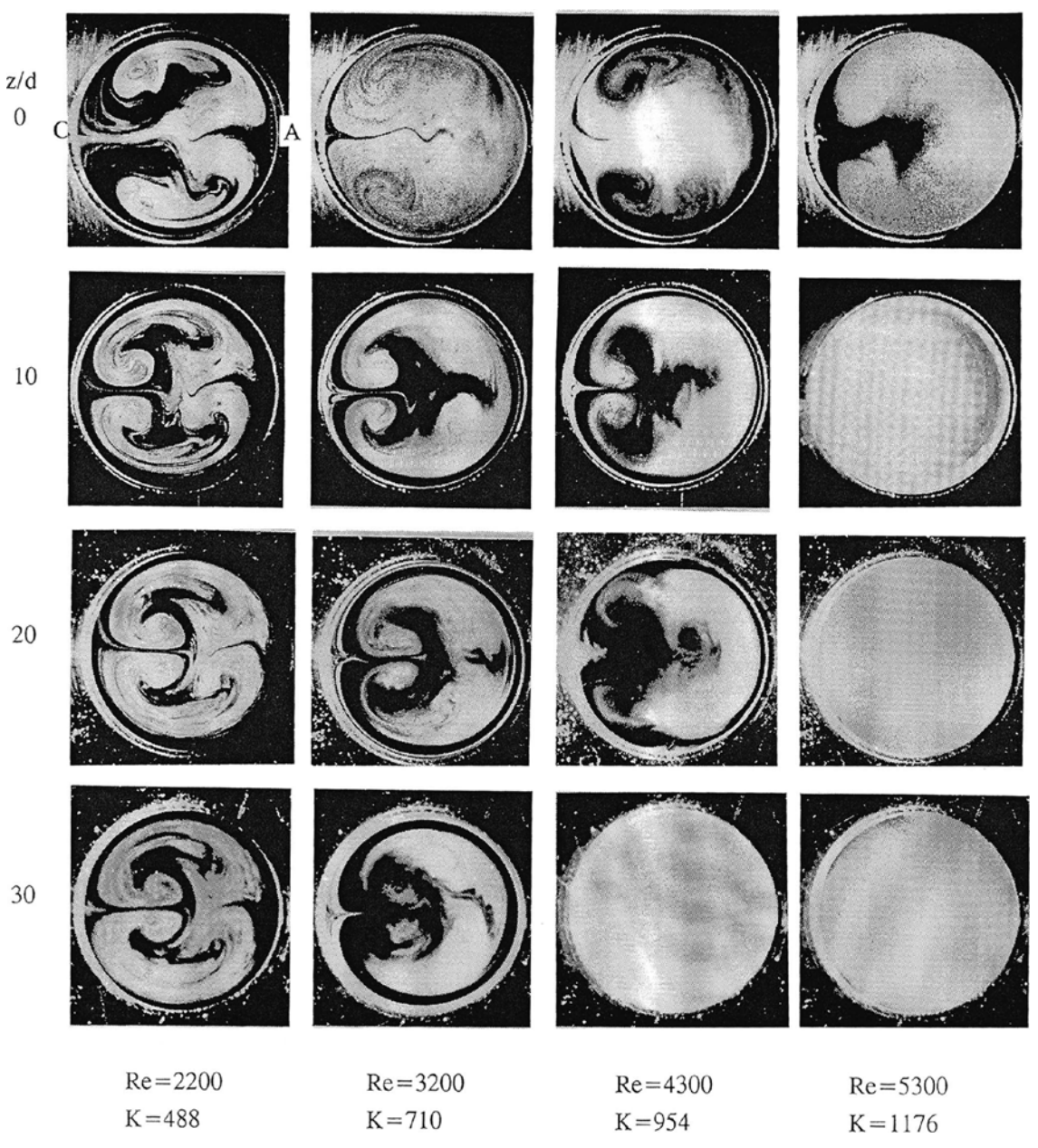

Fig. 6. The case of one-turn helical coil (360°).

The Case of 720° Coil (2-Turn Helically Coiled Pipe, $R_c\,\theta / d = 127.6$), Fig.7

At $z/d = 0$, the decrease of laminarization with the increase of Reynolds number is quite evident. The laminarization process is seen to be stronger near the inner wall. At $Re = 2200$ and 3200, the secondary flow pattern is very clear but becomes more complex. The developing secondary flow is quite symmetric with respect to the horizontal central axis. For $Re = 4300$ and 5300, the turbulent flow returns at $z/d = 30$ and 20, respectively. Figure 7 also shows clearly the usefulness of the simple smoke injection method for studying the relaminarization phenomena in helically coiled pipes. At $z/d = 0$, one sees the laminarization throughout the whole cross-section for $Re = 2200$ and 3200.

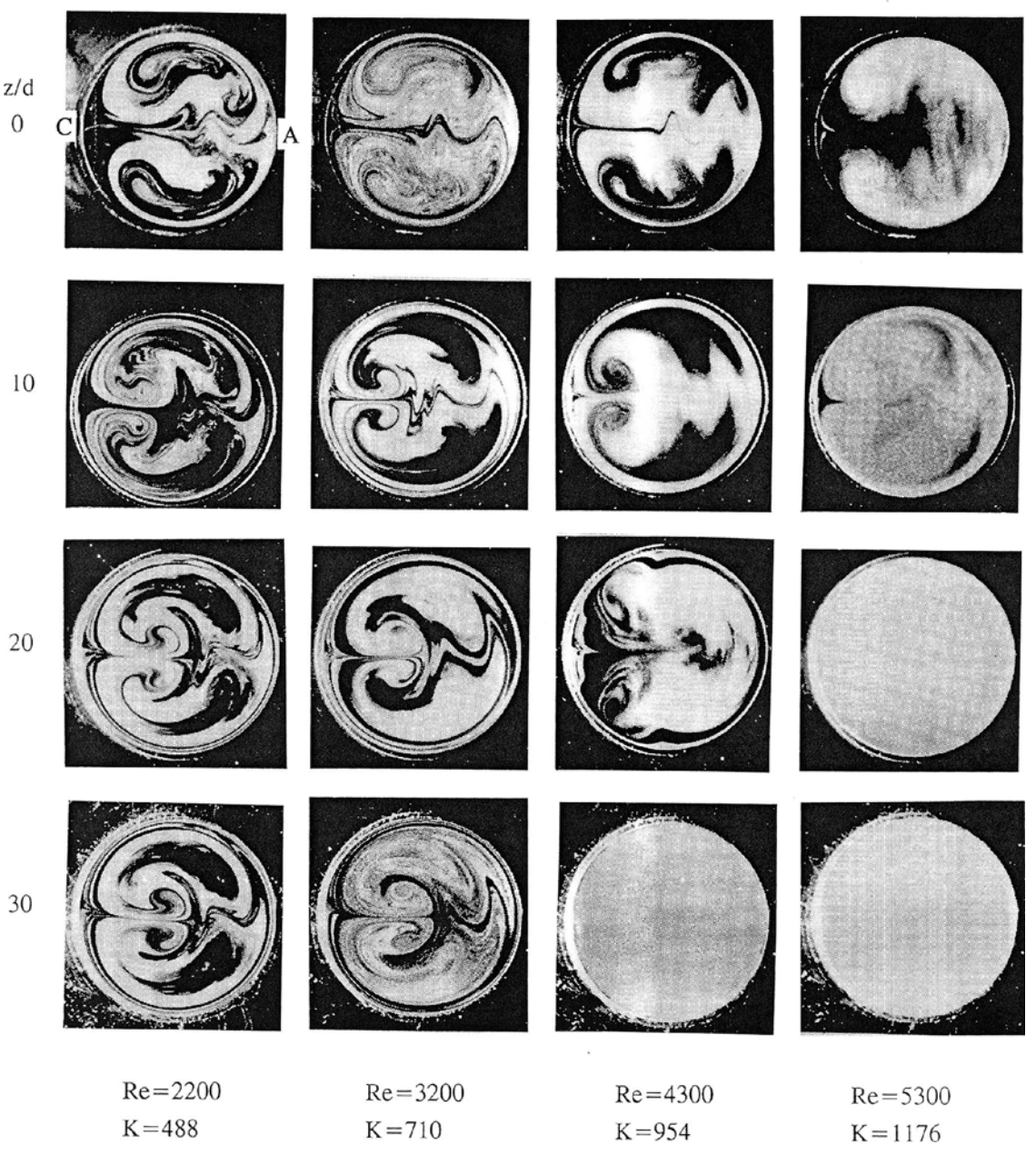

Fig. 7. The case of two-turn helical coil (720°).

The Case of 1800° Coil (5-Turn Helically Coiled Pipe, $R_e\theta / d = 319$), Fig.8

At *Re* = 2200 and 3200, the secondary flow pattern becomes very complex at the coil exit and in the downstream straight section. In the downstream section, one sees the interaction between the upper and lower regions and no symmetry of the flow pattern exists. The laminar boundary layer can be seen near the wall. At *z*/*d* = 0, the laminar flow may become fully developed.

At *Re* = 4300 and 5300, a weak secondary flow exists near the outer wall and the laminarization effect is quite small; the turbulent flow returns at *z*/*d* = 20 and 10, respectively. It is seen that the secondary flow pattern provides considerable insight into the laminarization phenomena in curved pipes.

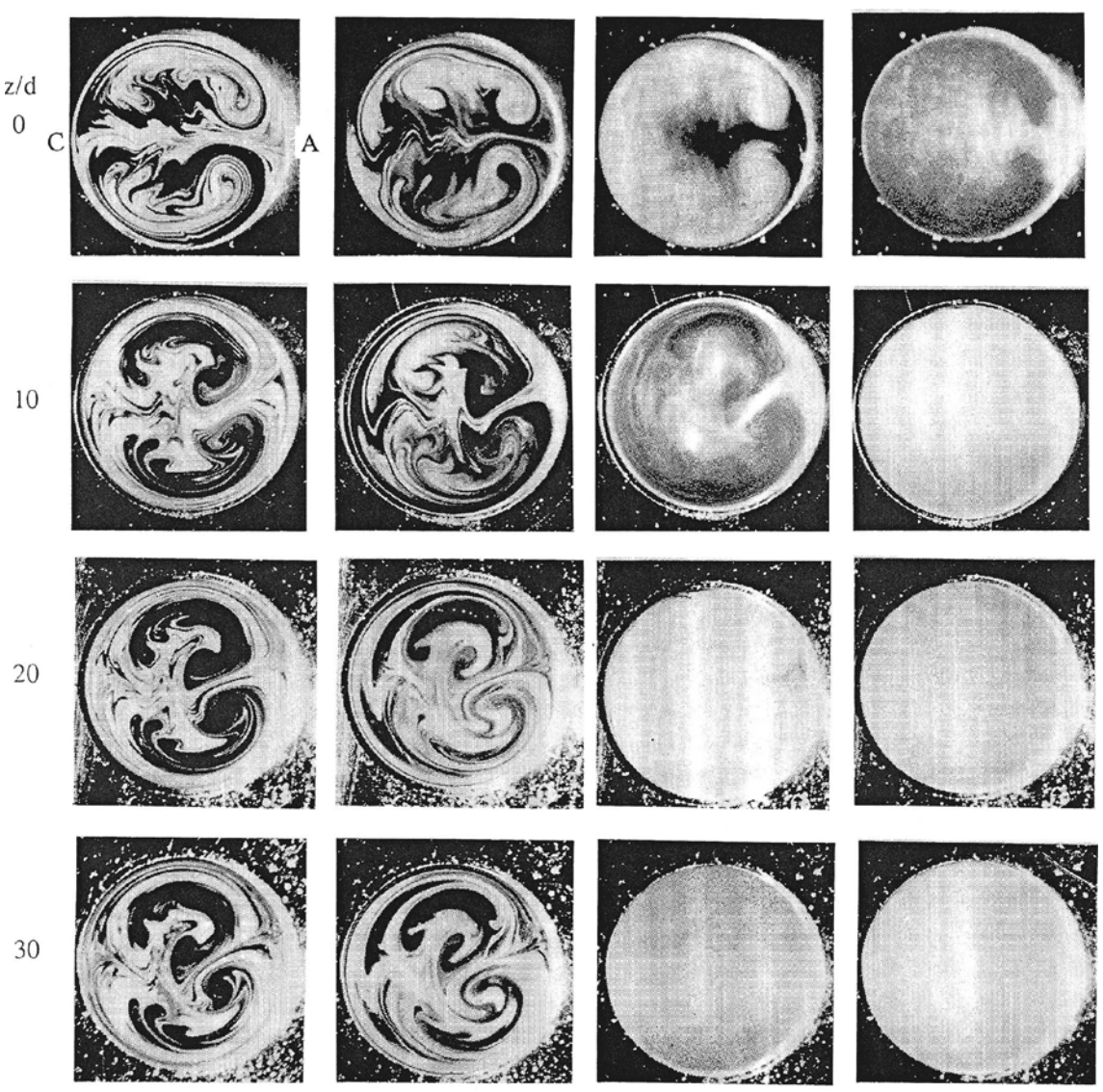

Fig. 8. The case of five-turn helical coil (1800°).

4.2 *The Effects of Dean Number on Distributions of the Local Turbulence Intensity and the Local Time-Mean Velocity Along the Horizontal Axis at the Exit Cross-Section of 180° Bend and 2-Turn Coil*

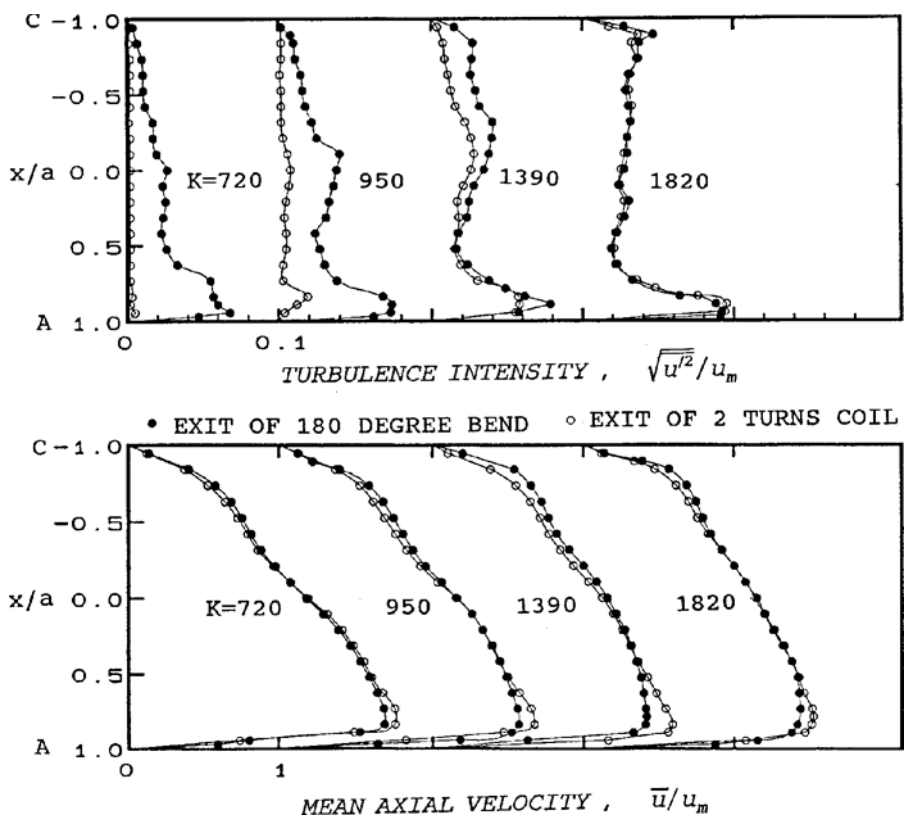

Fig. 9. Comparison of the developing turbulence intensity and mean axial velocity along the horizontal x-axis at the exit of 180° bend and 2-turn helical coil for Dean numbers K = 720, 950, 1390 and 1820.

Figure 9 shows the distributions of the axial mean velocity and the r.m.s. axial component of turbulent velocity, normalized by the mean velocity for the cases of Dean numbers K = 720, 950, 1390 and 1820 along the horizontal axis (A-C) at the exits of the 180° bend and the 2-turn coil. The time-mean axial velocity measurements show that the difference between the two profiles is relatively small and occurs near the outer wall. The velocity profile shows the known characteristic feature with the maximum velocity shifting towards the outer wall.

The turbulent intensity profiles show that the difference between the two cases decreases as the Dean number increases. At Dean number K = 1820, the difference is hardly discernible. One may conclude that at Dean number K = 1820, the flow may become fully developed at the exit of 180° bend. At K = 720, the turbulence intensity at the exit of the 2-turn coil is very small and the trend is similar at K = 950. When the turbulent intensity is very small, the flow regime may be steady laminar flow and the transition from turbulent to laminar flow occurs.

The distribution of the turbulence intensity for the case of 180° bend is of particular interest for K = 720, 950 and 1390. It is seen that the maximum turbulence intensity is located near the outer wall and its magnitude increases with the increase of Dean number. At K = 1820, the local maximum turbulence intensity is located near the inner wall for the case of 180° bend.

It is of special interest to observe that the maximum axial velocity near the outer wall for the case of 2-turn coil is always greater than that of the 180° bend. It is known that a flow acceleration decreases the magnitude of the fluctuations in the streamwise direction. It is thus seen that the maximum turbulence intensity near the outer wall for the 2-turn coil case is smaller than that of the 180° bend for K = 950 and 1390. This suggests that the laminarization process is stronger for the 2-coil case for K = 720, 950, and 1390. It is expected that after passing through more axial length of a helically coiled pipe, the turbulent flow becomes laminar if the entrance Reynolds number is less

than the critical value for a given curvature ratio.

At K = 1820, the turbulence intensity profiles for both cases are quite similar but a small difference between the velocity profiles near the inner and outer walls can be seen. And it seems that the laminarization will not occur at such a high Dean number with the corresponding Reynolds number Re = 8204 exceeding the critical Reynolds number Re_{cr} = 7600 based on equation (1). For $K \leq 1390$, the turbulence intensity for the 2-coil case is always lower than that of the 180° bend indicating clearly the laminarization process occurring in the 2-coil test section.

4.3 Development of Axial Mean Velocity and Turbulence Intensity in the Entrance Region of 180° Bend and the Downstream Straight Pipe for Re = 3200, 4300, 6300 and 8200, Figs. 10 to 13

The Case with Re = 3200 (K = 720), Fig.10

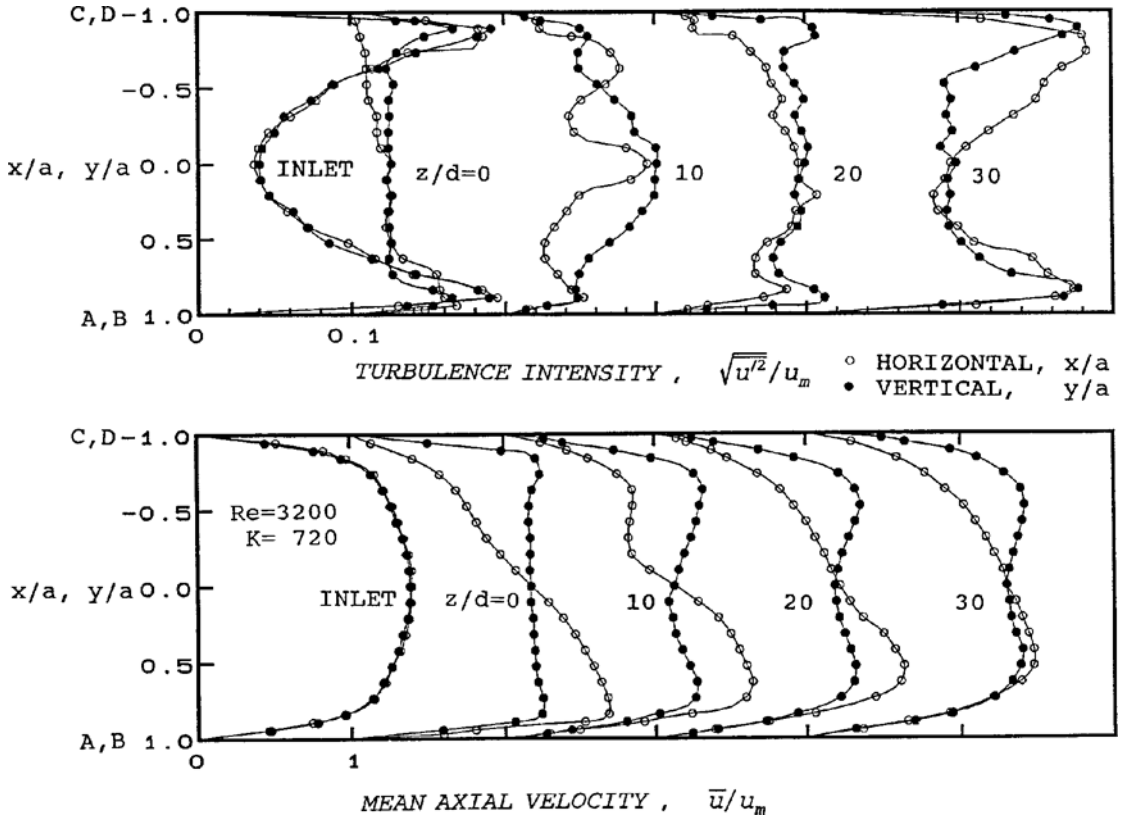

Fig. 10. Development of turbulence intensity and mean axial velocity along horizontal and vertical axes in 180° bend and downstream straight pipe at Re = 3200 (K = 720).

Figure 10 shows the axial distributions of the developing axial mean velocity and turbulence intensity along both horizontal (x/a) and vertical (y/a) centrelines in the entrance region (inlet and exit to the 180° bend) and in the downstream region with axial positions z/d = 0, 10, 20 and 30. The entry flow is fully developed turbulent flow. The differences in profiles for time-mean velocity and r.m.s. axial velocity fluctuations between the inlet and exit cross-sections represent the laminarization in the 180° bend. The entry turbulence intensity profiles along the horizontal and vertical axes show that the turbulence intensity reaches its largest value close to the wall. The two profiles are nearly identical along the x and y axes. It is known that the region of maximum turbulent kinetic energy production is found to lie near the maximum in turbulence intensity. Thus it seems that the turbulence intensity undergoes a substantial increase in the downstream direction due to the strong turbulence production therin.

The velocity profile along the horizontal x-axis shows the typical characteristic with the maximum velocity shifting toward the outer wall and the vertical symmetric profile shows a double-humped profile near the upper and lower walls. The velocity profiles at z/d = 0 (exit of 180° bend) show a definite characteristic of the curved pipe

flow. The distribution of the turbulence intensity at $z/d = 0$ reveals clearly the laminarization effect. Along the horizontal axis the turbulence intensity is rather small near the inner wall and increases only slightly in the core region reaching a maximum value near the outer wall. The profile along the vertical axis is nearly symmetric with respect to the tube centre; the value in the core region is small and the maximum value occurs near the upper and lower wall revealing the double humped profile. Flow visualization photograph in Fig.5 shows that the flow is still developing at $z/d = 0$.

The developing velocity profiles at $z/d = 10$, 20 and 30 retain the characteristic profile in a curved pipe flow with decreasing centrifugal force effect. The difference in two profiles decreases with the increase in distance. In the downstream region, the location of the maximum velocity moves gradually from the outer wall toward the pipe centre. This is the re-transition process and eventually the profile returns to a fully developed turbulent flow at a certain downstream position. The developing profile for the turbulence intensity in the downstream region is fairly complex.

At $z/d = 10$, the vertical distribution of the turbulence intensity is quite symmetric with respect to the pipe centre; the horizontal distribution shows the two minima and two maxima. The difference in magnitude between the two distributions is fairly large in the core region.

At $z/d = 20$, one sees the relaminarization effect near the inner wall but the maximum turbulence intensity is observed in the remaining wall region. In the core region, the difference in turbulence intensity between the two profiles is rather small. At $z/d = 30$, the relaminarization near the inner wall disappears and the turbulence intensity is fairly uniform in the centre region for vertical distribution. Both distributions exhibit maximum value near the wall and the gradual approach to a fully developed turbulent flow is seen. However, the fully developed condition is not reached yet. The behavior of the turbulence along the vertical and horizontal axes at $z/d = 10$, 20 and 30 is of particular interest.

The velocity profile changes appreciably from the entry flow to the exit flow at $z/d = 0$. Similarily the turbulent intensity at the bend exit ($z/d = 0$) is considerably reduced from that at the inlet of the bend. Especially, the turbulence intensity near the inner wall becomes very small and the flow near the inner wall may be considered as laminar. The change in profiles from the inlet to the exit of the bend represents the laminarization process.

The Case with Re = 4300 (K = 950), Fig.11

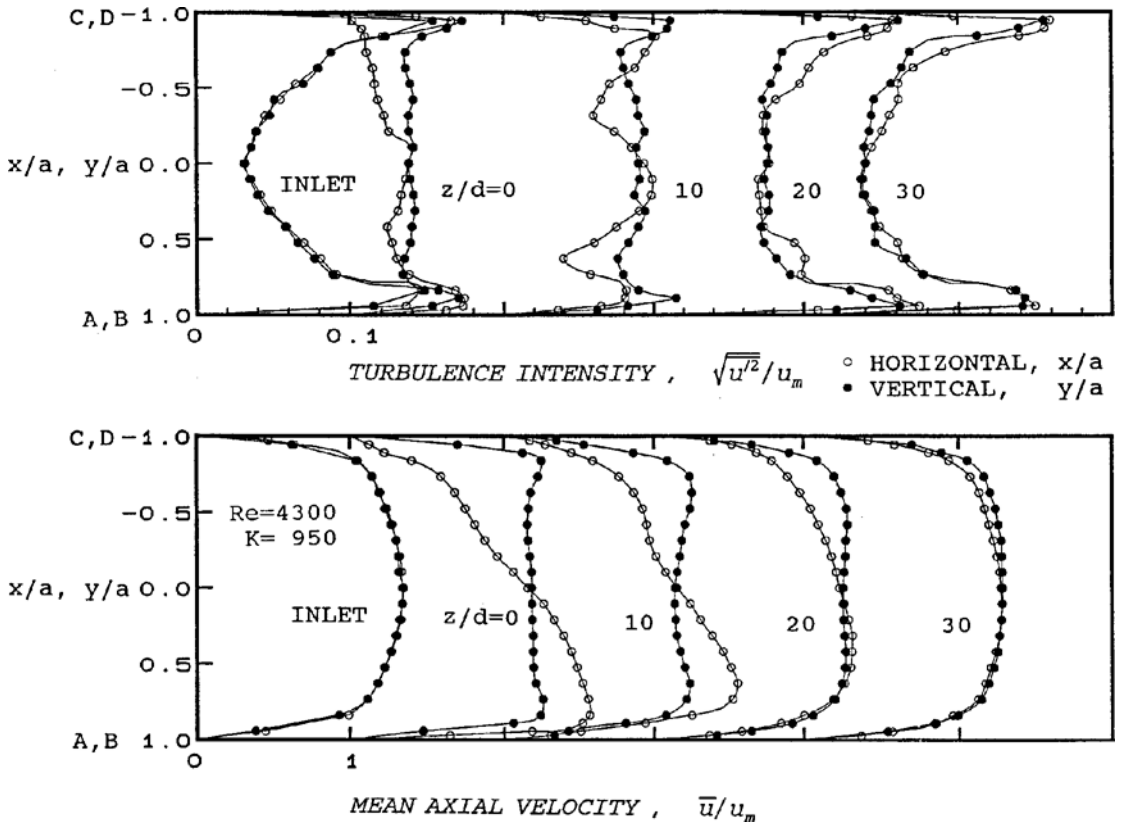

Fig. 11. The case with Re = 4300 (K = 950).

The general characteristics of the developing axial velocity and turbulence intensity in the entrance and downstream regions are somewhat different from those for the case with *Re* = 3200. The change in profiles for velocity and turbulence intensity from the entry to the exit flow in the 180˚ bend is quite appreciable indicating the laminarization effect in curved pipe. The developing velocity profiles at *z*/*d* = 0 show the effect of entry flow in the curved pipe. In the downstream region the maximum velocity near the outer wall gradually shifts toward the pipe center and at *z*/*d* = 30, the two profiles approach those of entry flow.

The profiles of turbulence intensities at *z*/*d* = 0 show clearly the laminarization with lower values in the core region. The region near the inner wall is relatively stable with lower turbulence intensity. At *z*/*d* = 10, the horizontal profile shows the two local minima. The profiles at *z*/*d* = 30 are seen to approach the entry profile. The turbulence intensity is larger near the wall.

The Case with Re = 6300 (K = 1390), Fig.12

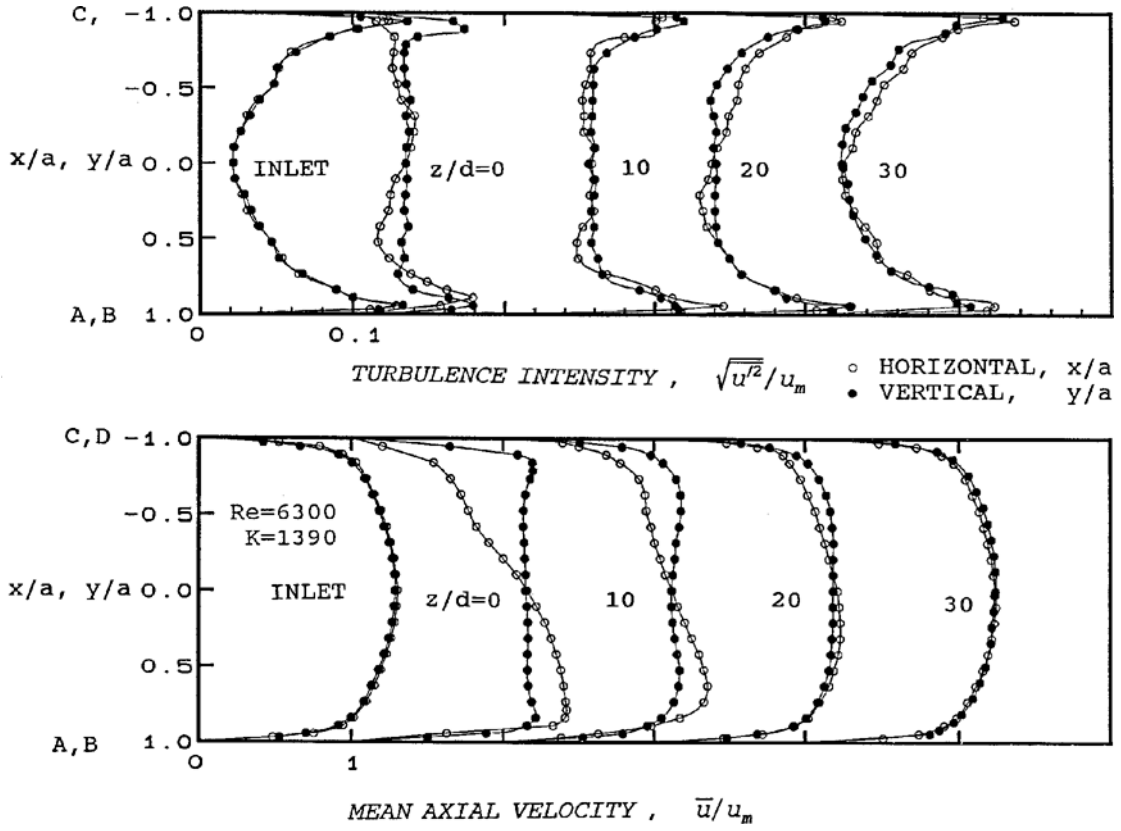

Fig. 12. The case with *Re* = 6300 (*K* = 1390).

The general trend for the velocity and turbulence intensity profiles at the inlet and exit of the 180˚ bend is similar to those at *Re* = 4300. The difference in profiles for turbulence intensity at *z*/*d* = 0 is quite small in the core region. At *z*/*d* = 30, the profiles for velocity and turbulence intensity almost approach entry profiles. Thus the development length in the downstream region becomes shorter at *Re* = 6300.

The Case with Re = 8200 (K = 1820), Fig.13

Based on Ito's criterion for critical Reynolds number for transition from laminar to turbulent flow in curved pipes, the entry flow to the 180˚ bend is considered to be fully developed turbulent flow. At the exit of the bend (*z*/*d* = 0), the turbulence intensity is uniform and small in the core region; the axial velocity profile along the vertical axis is quite uniform except the wall region. At *z*/*d* = 10, the difference in profiles for turbulence intensity exists near the outer and upper walls. At *z*/*d* = 30, the re-transition process is almost complete indicating a shorter downstream development length.

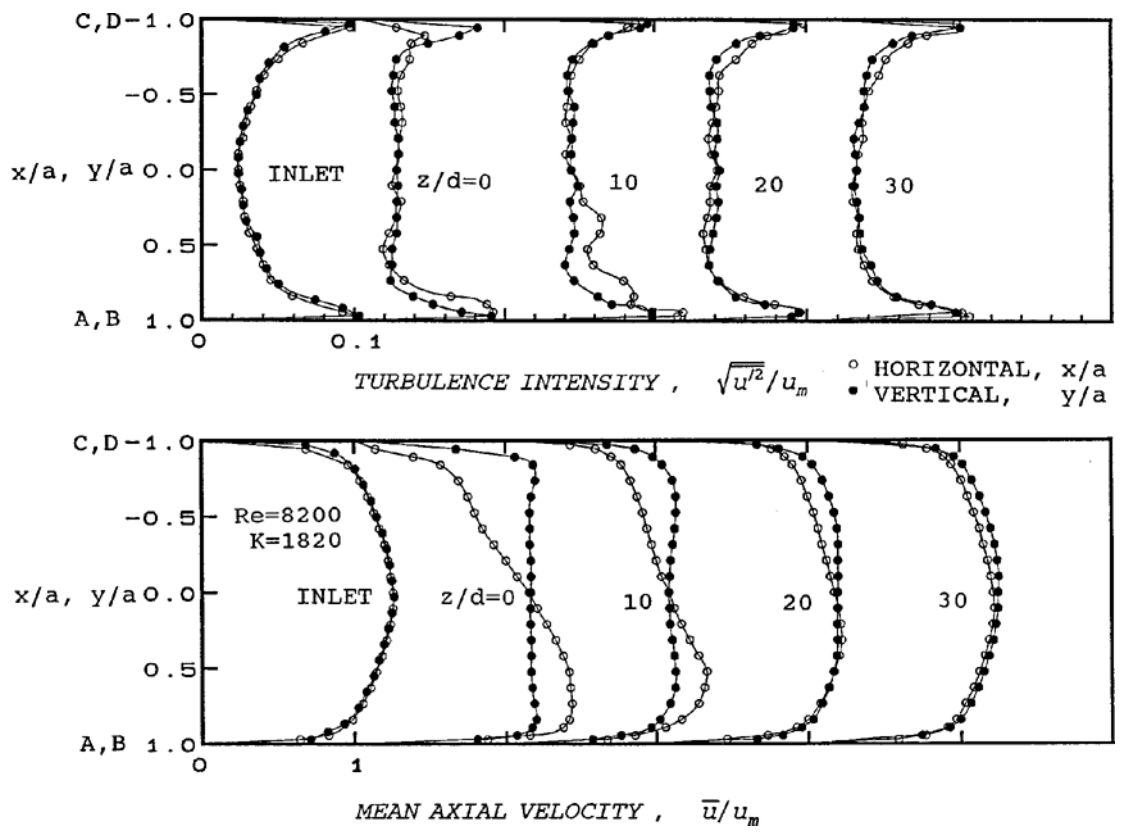

Fig.13. The case with *Re* = 8200 (*K* = 1820).

4.4 Time Records of the Fluctuating Velocity Field for Re = 3200, 4300, 6300 and 8200, Figs. 14 to 17

The Case with Re = 3200 (K = 720), Fig.14

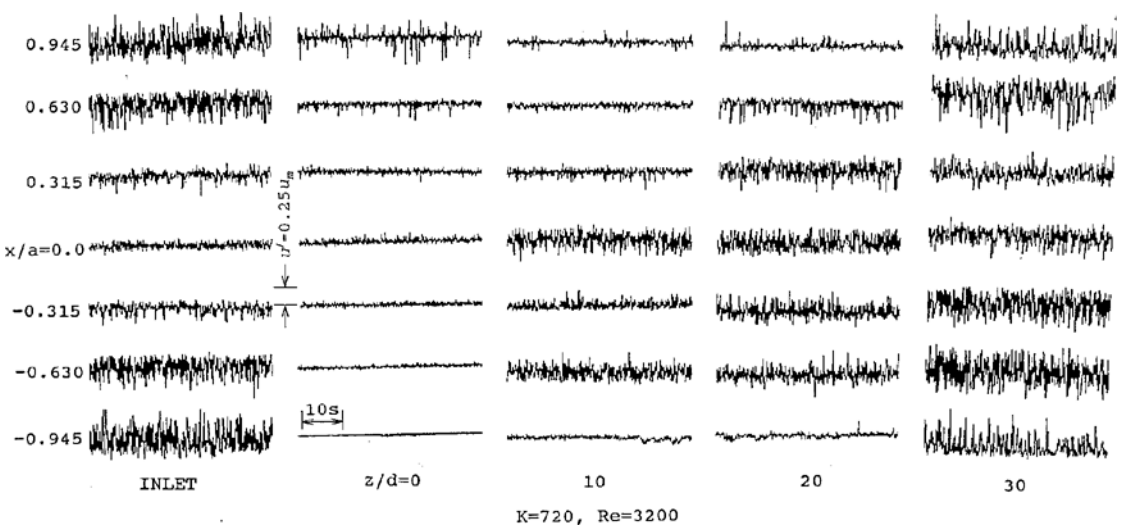

Fig. 14. Time traces showing the output of the hot-film sensor for fluctuating velocity at the inlet and exit of 180° bend and in the downstream section for *Re* = 3200 (*K* = 720).

Turbulent flow is characterized by the fluctuating velocity field. Figure 14 shows the instantaneous time traces of the fluctuating axial velocity along the horizontal x-axis at the inlet and exit ($z/d = 0$) of the 180° bend and at the downstream positions z/d = 10, 20 and 30 in the downstream straight pipe. The hot-film outputs at 7 horizontal positions for each measuring station are shown.

The distribution of the turbulence structure at the inlet of the bend confirms the turbulence level shown in Fig.10. At $x/a = \pm 0.945$ the turbulence level is higher near the wall and there is a substantial reduction in turbulence level observed at center ($x/a = 0$). At the exit of the bend, a drastic reduction in turbulence level occurs throughout the whole cross-section except the region near the outer wall ($x/a = 0.945$) indicating a substantial laminarization process caused by the developing secondary flow in the bend. In the downstream region, the laminarization process near the inner and outer walls at z/d = 10 and 20 is of special interest. *At* z/d = 30, the increase in the magnitude of the turbulent fluctuations is apparent and the flow recovers its turbulence level; the increase of turbulence level near the center over that of the inlet is noted.

The Case with Re = 4300 (K = 950), Fig.15

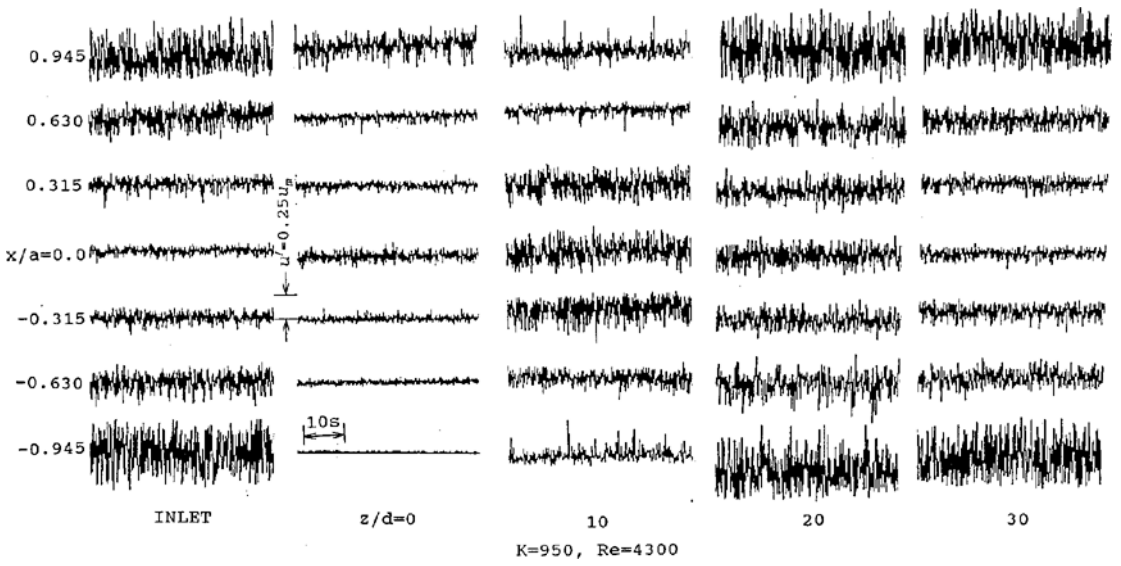

Fig. 15. The case with Re = 4300 (K = 950).

The trend of laminarization phenomena from the inlet to the exit ($z/d = 0$) of the bend is somewhat similar to the case with Re = 3200. It is seen that the flow is stable and laminar near the inner wall and unstable near the outer wall at $z/d = 0$. In the region near the tube centre the laminarization effect is evident. In the downstream region the amplification of disturbances occurs and results in the breakdown of laminar-like flow in the central region. It appears that the turbulent flow is recovered at z/d = 30. Basically one observes the re-transition laminar-turbulent flow in the downstream section. The changing fluctuating axial velocity at each horizontal position is very instructive in understanding the laminarization and re-transition phenomena for the present problem.

The Case with Re = 6300 (K = 1390), Fig.16

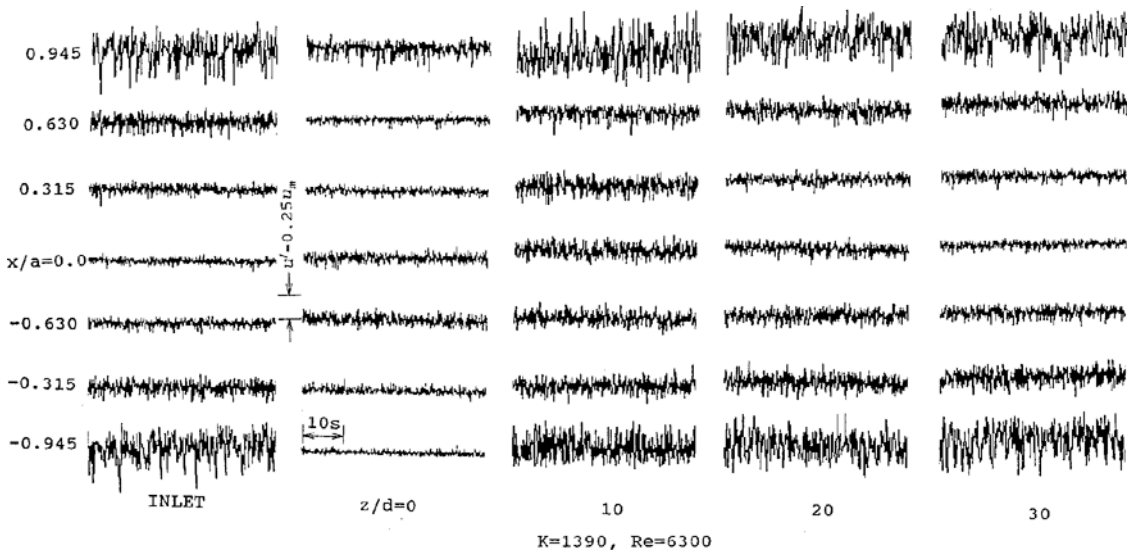

Fig. 16. The case with *Re* = 6300 (*K* = 1390).

The process of relaminarization near the inner and outer walls is quite evident and laminar-like flows may exist near the inner wall at $x/a = -0.945$. In the downstream section, the process of re-transition to turbulence is clearly illustrated. At $z/d = 30$, the re-transition process is nearly complete.

The Case with Re = 8200 (K = 1820), Fig.17

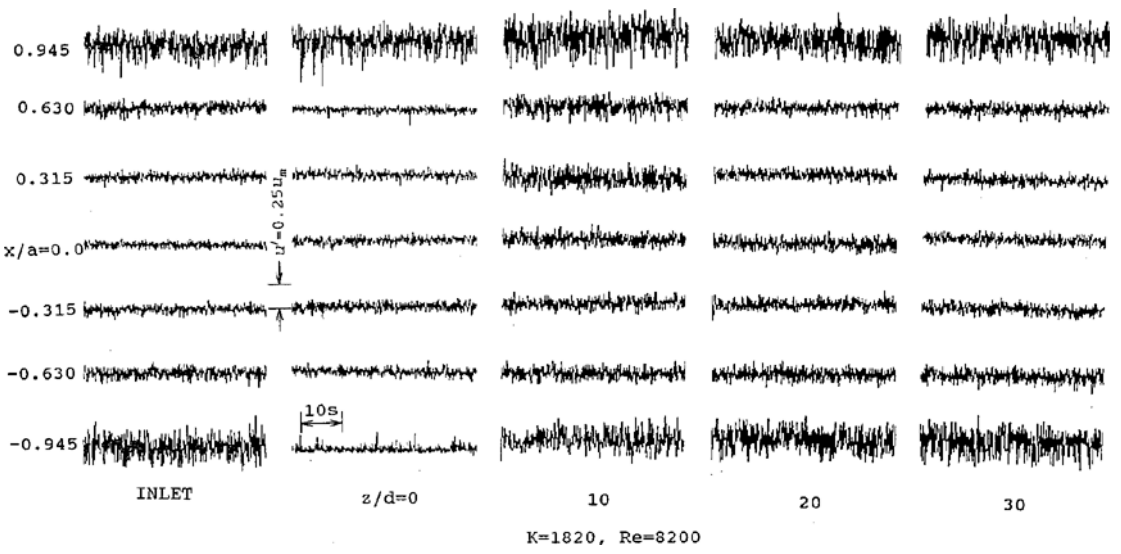

Fig. 17. The case with *Re* = 8200 (*K* = 1820).

As noted earlier, the entry flow to the 180° bend at *Re* = 8200 is considered to be fully developed turbulent flow. As can be seen from an overall examination of the changing fluctuating velocity between the inlet and exit of the bend at each position on the horizontal x-axis, laminarization brought about by centrifugal forces is relatively small. However, the laminarization is appreciable at $x/a = -0.945$ near the inner wall. This fact can also be observed from turbulence intensity distribution near the inner wall in Fig.13. In addition, it is apparent that re-transition to turbulent flow in the downstream section occurs more rapidly. At $z/d = 30$, the turbulent flow field appears to recover fully developed flow. In Fig.17, low amplitude, higher frequency disturbances dominate in core

region of the bend. For entry flow, high amplitude, higher frequency disturbances occur near the wall (x/a = ±0.945) and the same disturbances persist only at x/a = 0.945 in both the bend and the downstream section.

5. Concluding Remarks

Reynolds number has a destabilizing effect for flow in a straight pipe. On the other hand, secondary flow caused by centrifugal forces in a cross-section normal to the main flow in a curved pipe has a stabilizing effect delaying the laminar - turbulent transition. The relaminarization phenomena depend on Reynolds number and curvature ratio or Dean number. When inertial force is dominant over the centrifugal force, the re-transition from laminar to turbulent flow occurs. The prediction of transition from laminar to turbulent flow and the understanding of the relaminarization phenomena are important for flow in curved pipes and convective heat transfer problem. The critical Reynolds number for a curved pipe is higher than that for a straight pipe depending on the curvature ratio. Thus a fully developed turbulent flow in the upstream straight pipe becomes laminar in the coiled section in a certain range of Reynolds numbers, and the stabilizing effect of the coil persists to a certain degree in the downstream straight pipe.

In this investigation flow visualization using smoke injection method was used to study the relaminarization phenomena revealed by the cross-sectional view of the secondary flow in curved pipes. The effects of circular-arc bends (90° and 180°) and helical coils (1, 2 and 5 turns) on relaminarization phenomena in the curved section with a fully developed turbulent entry flow and the developing flow in the downstream straight pipe are studied by flow visualization for Reynolds numbers Re = 2200, 3200, 4300 and 5300.

The results of measurements for developing time-mean axial velocity and turbulence intensity in the 180° return bend and developing flow in the downstream straight pipe by means of a hot-film anemometer are presented. The entry flow to the bend is a fully developed, low Reynolds number turbulent air flow; the Reynolds numbers are Re = 3200, 4300, 6300 and 8200. The time traces showing the output of the hot-film sensor depicting the developing axial turbulence fluctuations are also presented for Reynolds numbers Re = 3200, 4300, 6300 and 8200. In the downstream section the re-transition process to turbulent flow occurs.

The stabilizing effect near the inner wall and the destabilizing effect near the outer wall of the 180° bend are confirmed by the turbulence intensity and the fluctuating velocity measurements. The maximum turbulence intensity near the wall is apparently related to the maximum turbulent kinetic energy production. The increase or decrease of the turbulence intensity in the central core region of the downstream straight pipe is probably due to transport of turbulent kinetic energy toward the centre-line from the region near the wall.

The behavior of turbulence intensity and velocity fluctuations together provide some insight into the relaminarization process in bends and coils and the re-transition process to turbulent flow in the downstream straight pipe. The degree by which turbulence is suppressed in the entrance region of the 180° bend is quite remarkable and depends on the Reynolds number and the curvature ratio. This can be seen readily from the difference in turbulence levels between the inlet and outlet of the 180° bend. The flow reacts rather quickly to the curvature effect in redistributing the turbulence intensity throughout the cross-section (see Figs.10 to 13). Although the time records of the velocity fluctuations along the vertical y-axis corresponding to those along the horizontal x-axis shown in Figs. 14 to 17 are not presented, the trends agree very well with the turbulence intensity data shown in Figs. 10 to 13. The redistribution of the turbulence level in the downstream section is due to transport process of turbulent kinetic energy.

The mean axial velocity distribution at the exit (z/d = 0) of the 180° bend shows a nearly linear distribution along the horizontal axis and a nearly uniform distribution along the vertical axis in the central core region (see Figs.10 to 13). The characteristic feature of the velocity profiles at z/d = 0 suggests that the profiles may be close to those of fully developed turbulent flow in curved pipes. Some aspects of the stabilization effects in flow through curved pipes and helically coiled pipes, and the destabilization effect for re-transition process in the downstream straight section are clarified in the present experimental investigation.

Acknowledgments

This work was supported by the Natural Sciences and Engineering Research Council of Canada through an operating grant.

References

Ackeret, J., Aspects of Internal Flow, Fluid Mechanics of Internal Flow, (1967); Sovran, G. (Ed.), Elsevier Publishing Co., New York, 1-26.

Akiyama, M., Murakoshi, T., Sugiyama, H., Cheng, K. C. and Nishiwaki, I., Numerical Solution of Convective Heat Transfer for Reverse Transition in the Bend Tube by a Low-Reynolds-Number Turbulent Model, JSME International Journal, Vol.31, No.2 (1988), 289-298.

Anwer, M., So, R. M. C. and Lai, Y. G., Perturbation by and Recovery from Bend Curvature of a Fully Developed Turbulent Pipe Flow, Physics of Fluids A, Vol.1 (1989), 1387-1397.

Bankston, C. A., The Transition from Turbulent to Laminar Gas Flow in a Heated Pipe, ASME Journal of Heat Transfer, Vol.92, (1970), 569-579.

Berger, S. A., Talbot, L. and Yao, L. S., Flow in Curved Pipes, Ann. Rev. Fluid Mech., Vol.15 (1983), 461-512.

Berger, S. A., Flow and Heat Transfer in Curved Pipes and Tubes, 29th AIAA Aerospace Sciences Meeting, (1991), AIAA 91- 0030.

Chang, S. M., Humphrey, J. A. C. and Modavi, A., Turbulent Flow in a Strongly Curved U-Bend and Downstream Tangent of Square Cross-Sections, PCH Physico-Chemical Hydrodynamics, Vol.4 (1983), 243-269.

Cheng, K. C. and Yuen, F. P., Flow Visualization Studies on Secondary Flow Patterns in Straight Tubes Downstream of a 180 deg Bend and in Isothermally Heated Horizontal Tubes, ASME Journal of Heat Transfer, Vol.109 (1987), 49-54.

Cheng, K. C., Takuma, M. and Kamiya, Y., Visualization of Developing Secondary Flow Patterns in the Hydrodynamic Entrance Region of a Curved Pipe, J. of Flow Visualization and Image Processing, Vol.2 (1995), 1-13.

Humphrey, J. A. C. and Webster, D. R., Questions in Fluid Mechanics - Reverse Transition Phenomena in Helically Coiled Pipes, ASME Journal of Fluids Engineering, Vol.115 (1993), 191-192.

Ishigaki, H., Analogy Between Turbulent Flows in Curved Pipes and Orthogonally Rotating Pipes, J. Fluid Mech., Vol.307 (1996), 1-10.

Ito, H., Friction Factors for Turbulent Flow in Curved Pipes, ASME Journal of Basic Engineering, Vol.81 (1959), 123-134.

Ito, H. and Miyakawa, T., Discharge Coefficients for 360 - Deg. Bend Flowmeters, Bulletin of the JSME, Vol.21 (1978), 1268-1276.

Ito, H., Flow in Curved Pipes, JSME International Journal, Vol.30 (1987), 543-552.

Kalb, C. E. and Seader, J. D., Entrance Region Heat Transfer in a Uniform Wall-Temperature Helical Coil with Transition from Turbulent to Laminar Flow, Int. J. Heat Mass Transfer, Vol.26 (1983), 23-32.

Lombardi, G., Sparrow, E. M. and Eckert, E. R. G., Experiments on Heat Transfer to Transpired Turbulent Pipe Flows, Int. J. Heat Mass Transfer, Vol.17 (1974), 429-437.

Nandakumar, K. and Masliyah, J. H., Swirling Flow and Heat Transfer in Coiled and Twisted Pipes, Advances in Transport Processes, (1986), John Wiley & Sons, 49-112.

Narasimha, R., The Three Archetypes of Relaminarization, Procs. 6th Canadian Congress of Applied Mechanics, Vancouver, (1977), 503-527.

Narasimha, R. and Sreenivasan, K. R., Relaminarization of Fluid Flows, Advances in Applied Mechanics, Vol.19 (1979), 221-309.

Ohadi, M. M. and Sparrow, E. M., Heat Transfer in a Straight Tube Situated Downstream of a Bend, Int. J. Heat Mass Transfer, Vol.32 (1987), 201-212.

Ohadi, M. M., Sparrow, E. M., Walavalkar, A. and Ansari, A. I., Pressure Drop Characteristics for Turbulent Flow in a Straight Circular Tube Situated Downstream of a Bend, Int. J. Heat Mass Transfer, Vol.33 (1990 a), 583-591.

Ohadi, M. M. and Sparrow, E. M., Effect of a 180 Degree Bend on Heat Transfer in a Downstream Positioned Straight Tube, Int. J. Heat Mass Transfer, Vol.33 (1990b), 1359-1362.

Patankar, S. V., Pratap, V. S. and Spalding, D. B., Prediction of Laminar Flow and Heat Transfer in Helically Coiled Pipes, J. Fluid Mech., Vol.62 (1974), 539-551.

Patankar, S. V., Pratap, V. S. and Spalding, D. B., Prediction of Turbulent Flow in Curved Pipes, J. Fluid Mech., Vol.67 (1975), 583-595.

Pennell, W. T., Eckert, E.R.G. and Sparrow, E. M., Laminarization of Turbulent Pipe Flow by Fluid Injection, J. Fluid Mech., Vol.52 (1972), 451-464.

Prandtl, L., The Mechanics of Viscous Fluids, W.F. Durand (ed.), Aerodynamic Theory, Vol.3 (1935), 155-162.

Rowe, M., Measurements and Computations of Flow in Pipe Bends, J. Fluid Mech., Vol.43 (1970), 771-783.

Sreenivasan, K. R., Laminarescent, Relaminarizing and Retransitional Flows, Acta Mechanica, Vol.44 (1982), 1-48.

Sreenivasan, K. R. and Strykowski, P.J., Stabilization Effects in Flow Through Helically Coiled Pipes, Experiments in Fluids, Vol.1 (1983), 31-36.

Sreenivasan, K. R., Some Studies of Non-Simple Pipe Flows, 8th Australasian Fluid Mechanics Conference, Procs., Vol.1 (1983), K 7.1-7.8.

Taylor, G.I., The Criterion for Turbulence in Curved Pipes, Proc. R. Soc., London, Ser. A, Vol.124 (1929), 243-249.

Torii, S. and Yang, W. J., Laminarization of Turbulent Gas Flow Inside a Strongly Heated Tube, Int. J. Heat Mass Transfer, Vol.40 (1997), 3105-3117.

Trefethen, L., Fluid Flow in Radial Rotating Tubes, Actes, IX, Congrès International de Mécanique Appliquée, Université de Bruxelles, Vol.2 (1957), 341-350.

Ward - Smith, A. J., Internal Fluid Flow, The Fluid Dynamics of Flow in Pipes and Ducts, (1980), Clarendon Press, Oxford.

White, C. M., Streamline Flow Through Curved Pipes, Proc. Roy. Soc., London, Ser. A, Vol.123 (1929), 645-663.

Wiswanath, P. R., Narasimha, R. and Prabhu, A., Visualization of Relaminarizing Flows, J. Indian Inst. Sci., Vol.60 (1978), p.159.